Polymer Journal
https://doi.org/10.1038/s41428-020-0373-2

ORIGINAL ARTICLE

Viscoelastic relaxation attributed to the molecular dynamics of polyrotaxane confined in an epoxy resin network

Akihiro Hanafusa[1] · Shota Ando[2] · Satoru Ozawa[1] · Masakazu Ito[1] · Ryuichi Hasegawa[1] · Koichi Mayumi[2] · Kohzo Ito[2]

Received: 15 March 2020 / Revised: 5 May 2020 / Accepted: 8 May 2020

Abstract

The molecular dynamics of polyrotaxane (PR) dispersed homogeneously in a cross-linked epoxy resin were studied using dynamic mechanical analysis (DMA) and pulsed NMR spectroscopy. In PR, poly-ε-caprolactone (PCL)-grafted α-cyclodextrins (CDs) are threaded on a polyethylene glycol (PEG) axis. At low temperatures, the PEG and PCL chains of the PR embedded in the epoxy network are in a glassy state. With increasing temperature, the PEG in the PR undergoes a glass-to-rubber transition and fluctuates in the glassy PCL-grafted CDs confined by the epoxy matrix, which causes viscoelastic relaxation. The glass transition temperature, T_g, of the PEG in the PR is much higher than that of pure PEG because of the strong confinement effect in the epoxy network. In addition, the T_g of the PEG drastically changes with coverage by the CDs on the PEG, suggesting that the topological constraint by the CDs also substantially influences the PEG dynamics. The viscoelastic relaxation ascribed to PEG enhances the deformability and toughness of the epoxy resin containing PR under uniaxial stretching.

Introduction

Polyrotaxane (PR) is a necklace-like supramolecular assembly in which ring molecules are threaded on an axial chain [1–5]. Because the ring molecules and the axial chain in PR are not covalently connected, the rings can slide on the axial chain under the topological constraints [6]. The sliding motion of the chain relative to the rings in PR solution has been used to develop molecular shuttles in which the ring slides between stations on the axial chain in response to external stimuli, such as pH and UV light [7]. Recently, PR has been utilized to fabricate tough polymer gels called slide-ring gels [5, 8, 9]. By cross-linking the rings of PRs in solution, the axial polymer chains are connected by figure-eight cross-links formed by two rings. The cross-links can slide on the axial polymer chains to homogenize the strand lengths between the cross-linking points, which enhances the deformability and toughness of the slide-ring gels [5, 9, 10]. The introduction of slidable cross-links toughens not only polymer gels but also rubbers containing no solvent [5, 11–14].

The relative motion between the axial chain and the ring molecules in PRs can also be observed in the glassy state. Kato et al. reported that PRs composed of polyethylene glycol (PEG) and methoxyethylated/hydroxypropylated α-cyclodextrin (CD) form an amorphous glass, called PR glass (Fig. 1a) [15–17]. As shown in Fig. 1a, PEG chains fluctuate in the glassy framework of methoxyethylated or hydroxypropylated CDs, and the motion of the PEG chains is similar to the reptation dynamics in the entanglement effect [16]. The local motion of the PEG confined in the CD framework causes a large viscoelastic subrelaxation at approximately −50 °C, which is close to the glass transition temperature of bulk PEG [16].

Supplementary information The online version of this article (https://doi.org/10.1038/s41428-020-0373-2) contains supplementary material, which is available to authorized users.

✉ Koichi Mayumi
koichi.mayumi@edu.k.u-tokyo.ac.jp

✉ Kohzo Ito
kohzo@edu.k.u-tokyo.ac.jp

[1] Materials Characterization Laboratory, Science & Innovation Center, Mitsubishi Chemical Corporation, 1000 Kamoshida-cho, Aoba-ku, Yokohama, Kanagawa 227-8502, Japan

[2] Material Innovation Research Center (MIRC) and Department of Advanced Materials Science, Graduate School of Frontier Sciences, The University of Tokyo, 5-1-5 Kashiwanoha, Kashiwa, Chiba 277-8561, Japan

Published online: 12 June 2020

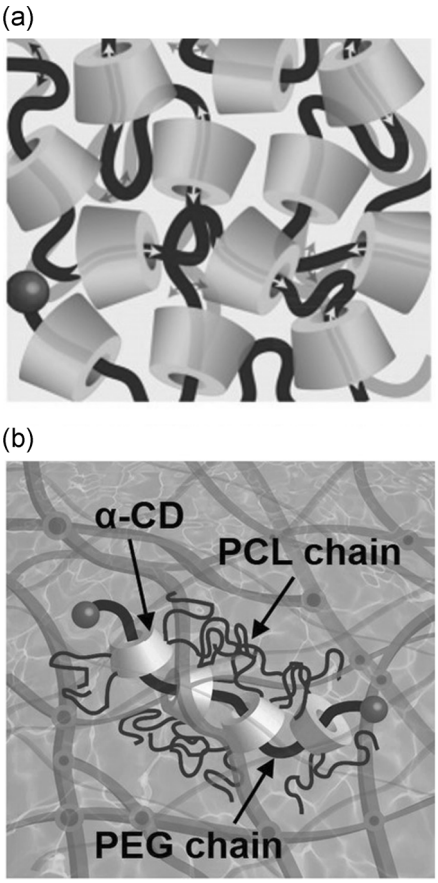

Fig. 1 Schematics of (**a**) PR glass [14] (reprinted with permission from Journal of Physical Chemistry Letters. Copyright (2015) American Chemical Society) and (**b**) PCL-grafted PR in epoxy resin

Recently, PRs have been introduced into epoxy resins to increase their mechanical toughness [18–21]. Epoxy resins have various applications, such as in coatings, adhesives, fiber composites, and integrated circuits, because of their advantages of excellent mechanical strength, adhesion, heat resistance, electrical insulation, chemical resistance, and water resistance [22–24]. However, the toughness of epoxy resins is poor and needs to be improved. Naito et al. found that poly-ε-caprolacton (PCL)-grafted PR can be homogeneously dispersed into cross-linked epoxy resins (Fig. 1b) and that the introduction of PCL-grafted PR enhances the fracture toughness and adhesion strength of the resin [20]. The toughening may be caused by the molecular dynamics of PCL-grafted PR in the epoxy network. The epoxy resin containing PCL-grafted PR shows a unique viscoelastic relaxation between 50 °C and 150 °C [20]. Because the strength of the viscoelastic relaxation increases with the content of PCL-grafted PR, the unique viscoelastic relaxation can be attributed to the molecular dynamics of the PCL-grafted PR [20], but the detailed molecular mechanism has not yet been clarified.

In this study, we investigated the molecular dynamics of PCL-grafted PR in epoxy resins by dynamic mechanical analysis and pulsed NMR spectroscopy to reveal the molecular origin of the unique viscoelastic relaxation. As shown in Fig. 1b, the PCL-grafted PR is isolated and confined by the epoxy network. An interesting question here is how different the molecular dynamics of PCL-grafted PR trapped in the epoxy network are from those of PR glasses shown in Fig. 1a. In addition, to determine the dominant features of the PR dynamics responsible for the viscoelastic relaxation, we compared epoxy resins containing PCL-grafted PRs with different coverages of CDs on the PEG. Finally, we performed tensile experiments on the epoxy resins with PCL-grafted PRs at different temperatures and analyzed the relationship between the viscoelastic properties and the large deformation stress-strain behaviors.

Experimental section

Materials

Diglycidyl ether of bisphenol A (DGEBA) and 4,4'-diaminodiphenylmethane (DDM) were used as the monomer and curing agent of the matrix resin, respectively. DGEBA (grade name: jER828, epoxide equivalent weight: 184–194 g/mol) was provided by Mitsubishi Chemical Corporation. DDM (amine hydrogen equivalent weight: 49.6 g/mol) was purchased from TCI Chemicals, Japan.

As shown in Fig. 2, we prepared four types of epoxy resins: a neat epoxy resin, an epoxy resin containing PCL-grafted PR with 28% CD coverage (epoxy/PR28), an epoxy resin containing PCL-grafted PR with 9% CD coverage (epoxy/PR09), and an epoxy resin containing linear PCL (epoxy/PCL). PR28 and PR09 are composed of hydroxypropylated α-CD with PCL graft chains and PEG. PR28 (grade name: SH2400P) was provided by Advanced Soft Materials Inc., Japan. For PR28, the number average molecular weight (M_n) of the PR, the M_n of PEG, the coverage ratio of CD on the PEG, the number of hydroxypropyl groups per CD unit, the monomer number of the PCL graft chains, and the number of PCL graft chains per CD were 314 kg/mol, 20,000 g/mol, 28%, 7.8, 9.8, and 8.4, respectively. PR09 was prepared according to a previously reported procedure [25]. For PR09, the number average molecular weight (M_n) of the PR, the M_n of PEG, the coverage ratio of CD on PEG, the number of hydroxypropyl groups per CD unit, the monomer number of the PCL graft chains, and the number of PCL graft chains per CD were 310 kg/mol, 30,000 g/mol, 8.5%, 3.3, 15 and 5.0, respectively. For epoxy/PCL, PCL with a M_n of

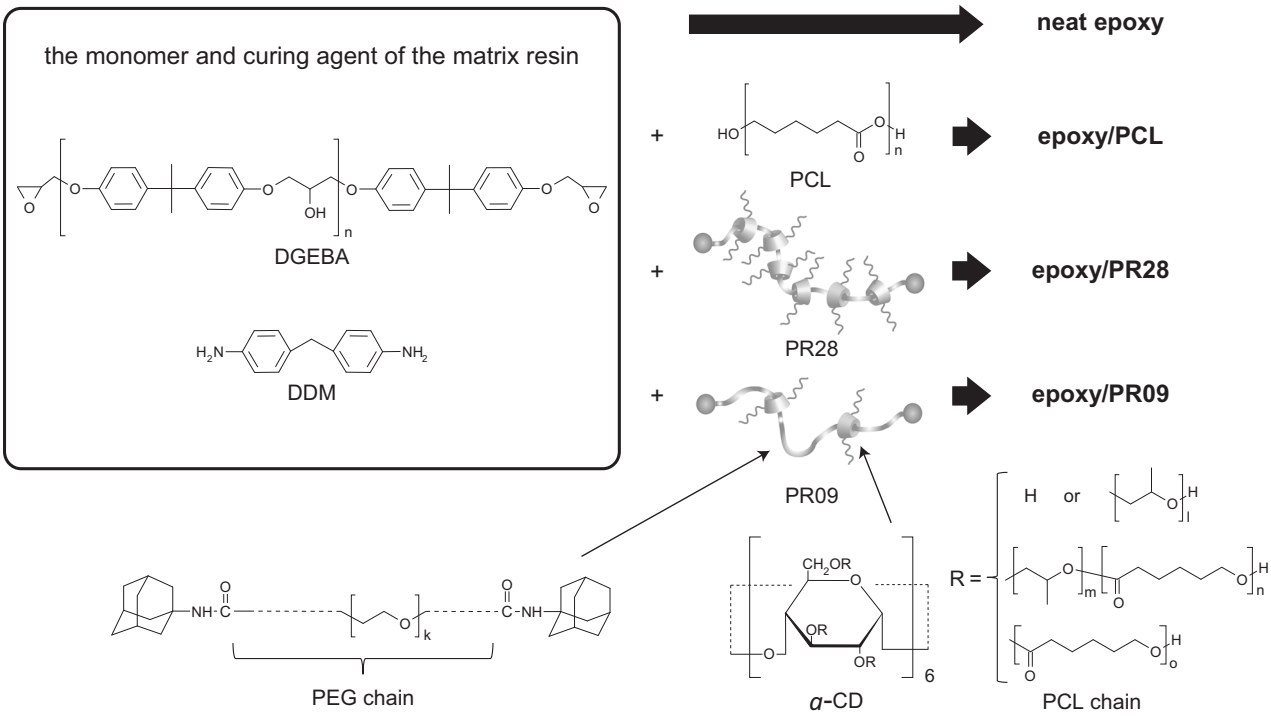

Fig. 2 Chemical structures and schematics of the samples

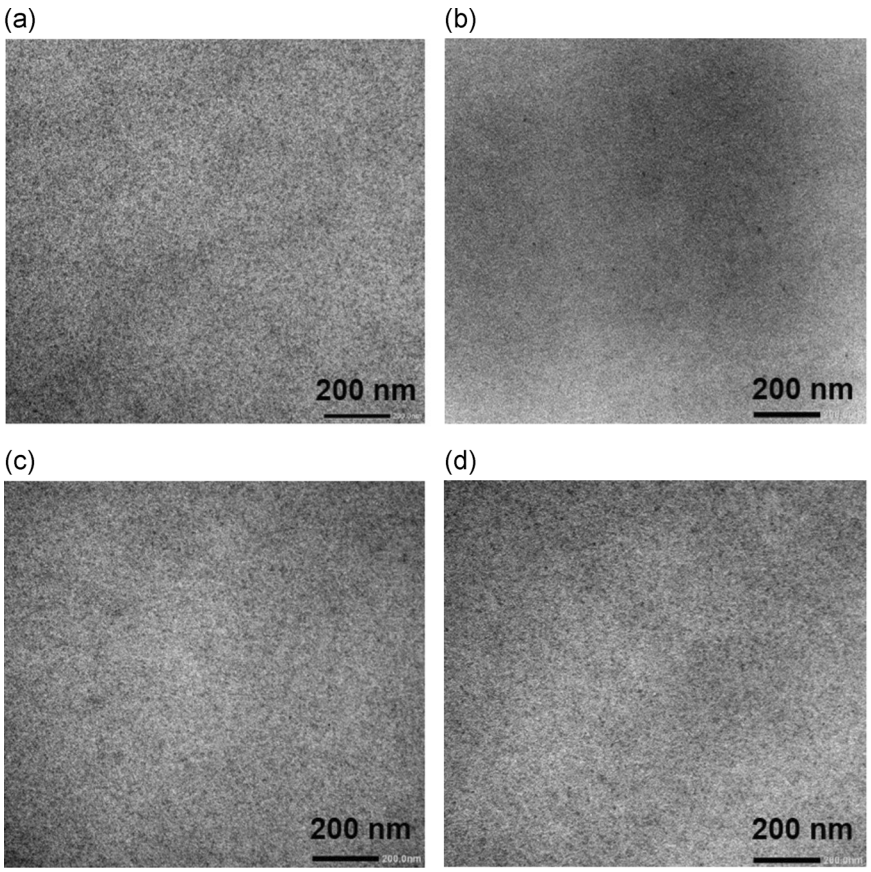

Fig. 3 TEM images of cured samples observed after staining with RuO_4: (**a**) neat epoxy, (**b**) epoxy/PCL, (**c**) epoxy/PR28, (**d**) and epoxy/PR09

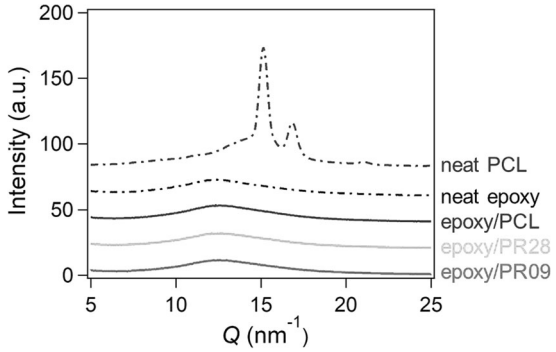

Fig. 4 WAXS profiles of neat PCL, neat epoxy, epoxy/PCL, epoxy/PR28, and epoxy/PR09

70,000–90,000 g/mol was purchased from TCI Chemicals, Japan.

Preparation of the epoxy resin

Cured epoxy specimens containing the PRs (epoxy/PR28 and epoxy/PR09) were prepared by the following procedure: PR28/PR09 (0.4 g) was added to DGEBA (4.0 g), and the mixture was stirred at 90 °C for 30 min. Next, DDM (1.16 g) was added to the blends and mixed at 85 °C for 15 min. The mixture was poured into a dumbbell-shaped silicone mold (JIS K 6251, 1 mm in thickness) for tensile experiments and a square silicone mold ($5 \times 30 \times 1$ mm^3) for the other measurements and degassed at 85 °C for 15 min. For the curing reaction, the mixture was heated at 90 °C for 15 min and then at 150 °C for 2 h to obtain transparent cured epoxy specimens. For epoxy/PCL, the mixture of PCL (0.4 g) and DGEBA (4.0 g) was stirred at 160 °C for 30 min. The rest of the procedure for preparing epoxy/PCL was the same as that for epoxy/PR28 and epoxy/PR09. Neat epoxy specimens were obtained in the same way.

TEM

Transmission electron microscopy (TEM) images of the epoxy specimens were obtained using a JEOL JEM-1400F instrument at an acceleration voltage of 80 kV at room temperature. The TEM images were obtained in bright-field mode. Ultrathin specimens were prepared using a Leica EM UC7 ultramicrotome and transferred onto copper grids. The specimens were stained with ruthenium tetroxide (RuO_4) vapor.

WAXS

Wide-angle X-ray scattering (WAXS) measurements were performed on a Rigaku NANOPIX using Cu Kα radiation at a generator power of 40 kV and 30 mA at room temperature. The exposure time for each measurement was 10 s. The obtained two-dimensional scattering patterns were converted to scattering profiles, with circular averaged intensity versus amplitude of scattering vector $Q = 4\pi\sin(\theta/2)/\lambda$, where θ is the scattering angle and λ is the wavelength of the incident X-ray.

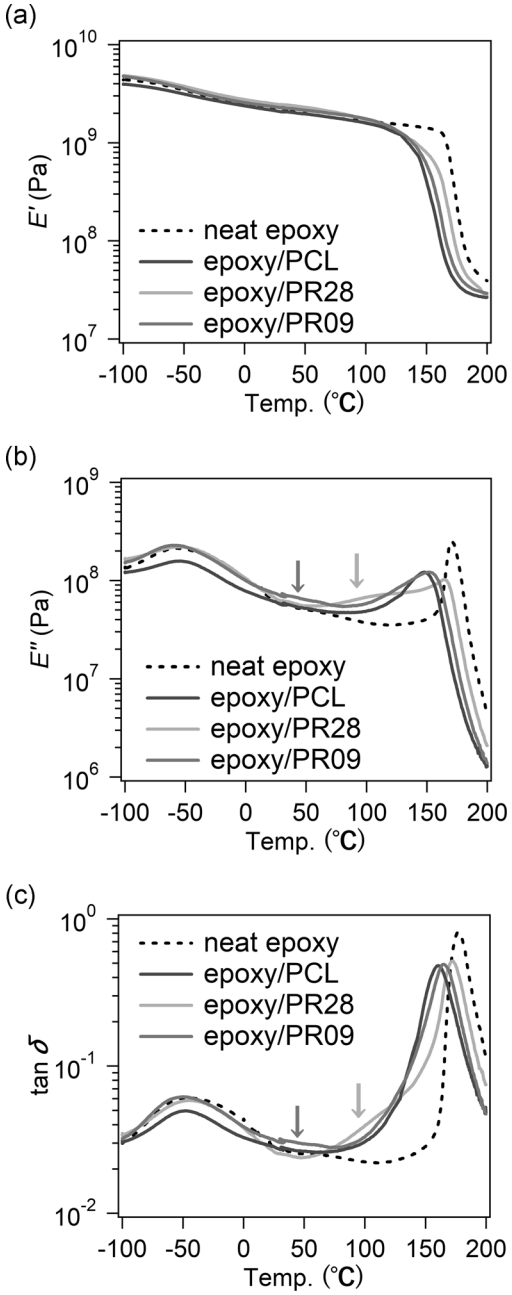

Fig. 5 Temperature dependence of the (**a**) storage modulus (*E'*), (**b**) loss modulus (*E''*), and (**c**) loss tangent (tan δ) for the neat epoxy resin, epoxy/PCL, epoxy/PR28 and epoxy/PR09

DMA

Dynamic mechanical analysis (DMA) measurements were performed using a Metravib DMA + 300 with a tension mode at 3 °C/min from −100 °C to 200 °C. Cured

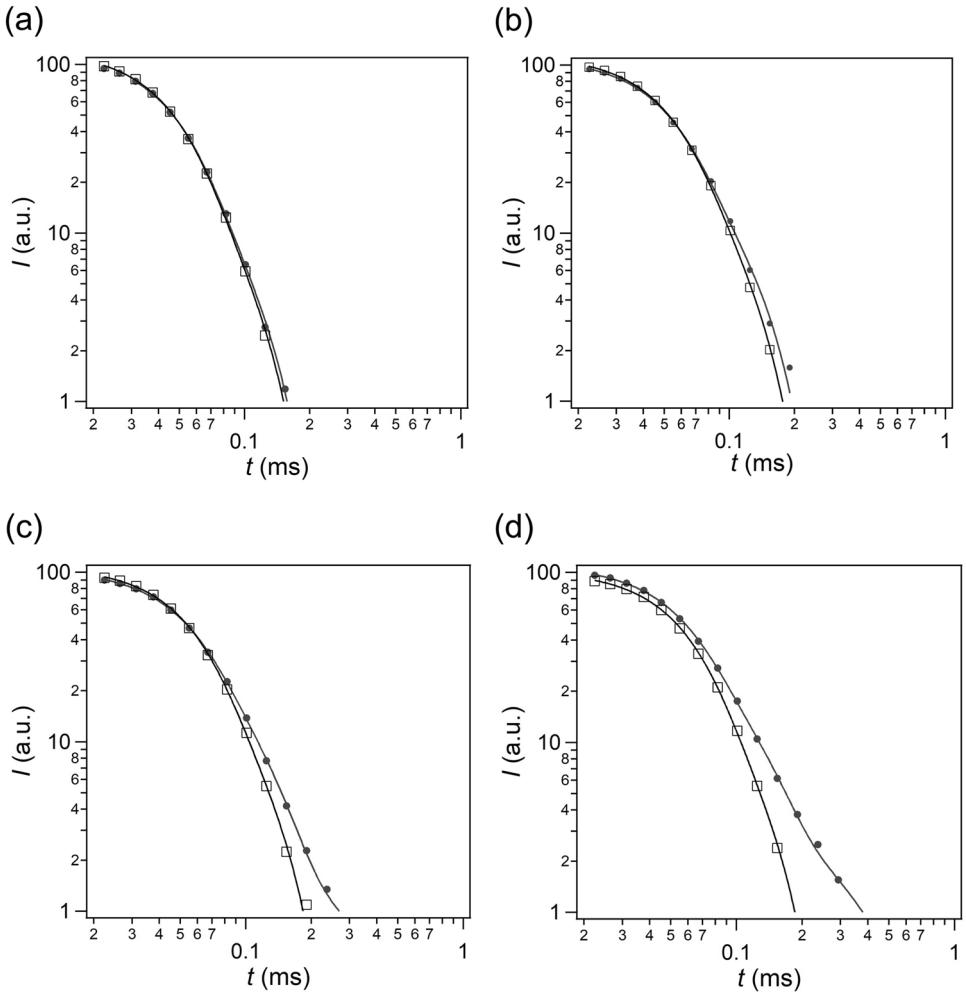

Fig. 6 FIDs of neat epoxy (open squares) and epoxy/PCL (filled circles) at (**a**) 30 °C, (**b**) 90 °C, (**c**) 120 °C, and (**d**) 150 °C. The solid lines are fitting results with Eq. 1 or 2

specimens with dimensions of 5 mm (width) × 30 mm (length) × 1 mm (thickness) were used. The frequency and strain were fixed at 2 Hz and 0.2%, respectively.

Pulsed NMR spectroscopy

Pulsed NMR spectra were acquired using a Bruker Minispec mq20 (20 MHz). Each sample (~300 mg) was loaded into a glass NMR sample tube. The proton spin-spin relaxation time (T_2) measurements were carried out using the solid-echo pulse sequence. For neat PCL, the spin-echo pulse sequence was also used above 60 °C. The temperature was changed at intervals of 30 °C from −90 °C to 210 °C. The number of scans and measurement time were 64 and 33 min, respectively.

Uniaxial tensile tests

Uniaxial tensile tests of the epoxy specimens were carried out on a Shimadzu autograph AG-100 KNG with a 100 kN load cell at room temperature and at 90 °C. Dumbbell-shaped specimens with dimensions of 4 mm (width) × 16 mm (length of the straight area) × 1 mm (thickness) were used. The initial distance between the crossheads was 25 mm, and the crosshead speed was 1 mm/min. Tensile tests at 90 °C were conducted inside a thermostatic chamber (TCR2-300).

Results and discussion

TEM

TEM measurements were performed to observe the dispersion of PCL, PR28, and PR09 in the epoxy resin. As shown in Fig. 3, the TEM images of epoxy/PCL, epoxy/PR28, and epoxy/PR09 are almost the same as that of the neat epoxy resin, and no dark domains of PCL, PR28, and PR09 are observed. This result indicates that all the additives (PCL, PR28, and PR09) are homogeneously dispersed in the epoxy network, which is consistent with a previous work [20].

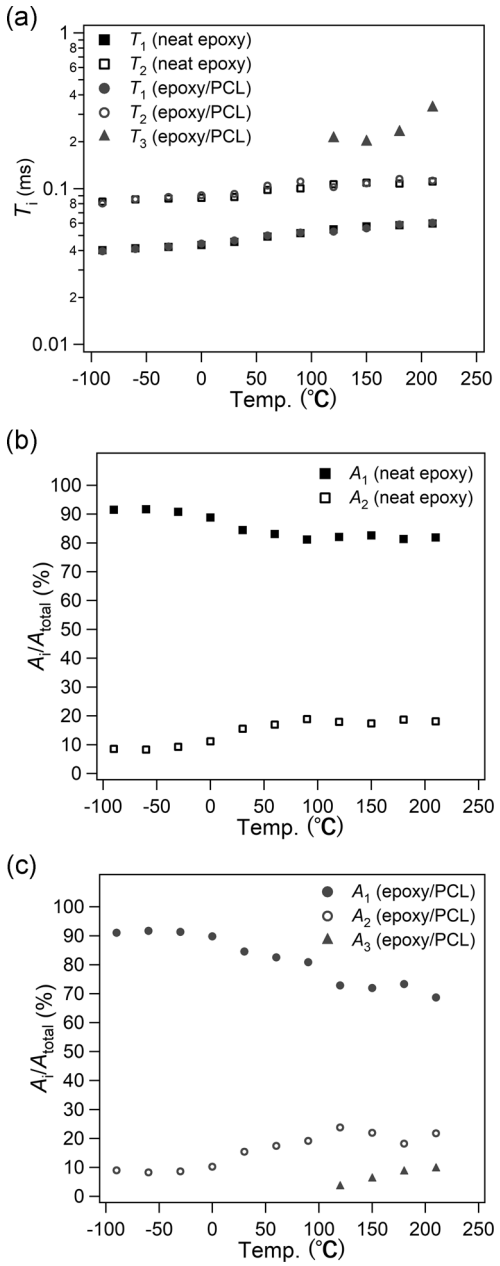

Fig. 7 Temperature dependence of (**a**) relaxation times T_i ($i = 1, 2, 3$) for the neat epoxy resin and epoxy/PCL, (**b**) A_i/A_{total} ($i = 1, 2$) for the neat epoxy resin, and (**c**) A_i/A_{total} ($i = 1, 2, 3$) for epoxy/PCL

WAXS

Figure 4 shows the WAXS profiles of neat PCL, neat epoxy resin, epoxy/PCL, epoxy/PR28, and epoxy/PR09 at room temperature. For the neat PCL, two sharp diffraction peaks were observed at $Q = 15.0$ and 16.6 nm^{-1} corresponding to the (110) and (200) planes of the PCL crystals [12]. The neat epoxy resin shows a broad amorphous halo, which is attributed to the correlation between the components of the epoxy resin [26–28]. The WAXS profiles of epoxy/PCL, epoxy/PR28, and epoxy/PR09 are the same as that of the neat epoxy resin, and no sharp peaks of PCL crystals are present. The crystallization of the PCL chains is suppressed in the epoxy network. This is consistent with the DSC (Fig. S1) and TEM results showing that PCL, PR28, and PR09 are homogeneously dispersed and confined by the epoxy network.

DMA

The viscoelastic properties of the epoxy resins were measured using DMA. Figure 5 shows the temperature dependence of the storage modulus (E'), loss modulus (E''), and loss tangent (tan δ) for the neat epoxy resin, epoxy/PCL, epoxy/PR28, and epoxy/PR09. For the neat epoxy resin, a sharp decrease in E' corresponding to the glass-rubber transition occurred at ~170 °C, and a broad peak for tan δ was observed from −100 °C to 0 °C. The subrelaxation in the low-temperature regime is attributed to local motion in the epoxy resins [29–31], which is not influenced by the introduction of PCL, PR28, and PR09 to the epoxy network. The addition of PCL, PR28, and PR09 to the epoxy resin decreases the glass transition temperature (T_g). Based on their E'' peaks, the α-relaxation temperatures of the neat epoxy resin, epoxy/PCL, epoxy/PR28, and epoxy/PR09 were determined to be 171 °C, 148 °C, 164 °C and 152 °C, respectively. The relaxation temperature of epoxy/PR28 is higher than that of epoxy/PCL and close to that of the neat epoxy resin, as shown in a previous report [20]. Similar trends were observed in the T_g values determined by DSC and DMA (see Sections S1 and S2 in the Supporting information).

The effects of the additives on the viscoelastic properties of the epoxy resins are clearly visible in the intermediate temperature range from 0 °C to 150 °C (Fig. 5). For epoxy/PCL, tanδ increases rapidly at 100 °C, and the viscoelastic relaxation may be a result of the addition of PCL. In the case of epoxy/PR28, tan δ starts to increase at 60 °C, and an additional broad relaxation from 60 °C to 100 °C is observed only in epoxy/PR28 (green arrow in Fig. 5c), which is consistent with a previous study [20]. Because the strength of the viscoelastic relaxation increases with increasing concentration of PR28 [20], the unique relaxation may be related to the molecular dynamics of PR28 in the epoxy network. Considering that the molecular mobility of PR should be enhanced by reducing the coverage of CD on PEG, we measured the viscoelastic properties of epoxy/PR09. Interestingly, for epoxy/PR09, the unique relaxation typical for epoxy/PR28 (60 °C to 100 °C) disappears, and instead a weak additional relaxation is observed in a lower temperature range (from 20 °C to 70 °C, red arrow in Fig. 5c). The reduction of the coverage in PR decreases the temperature of the excess viscoelastic relaxation, which indicates that the molecular dynamics of PR in the epoxy network become faster with decreasing PR coverage.

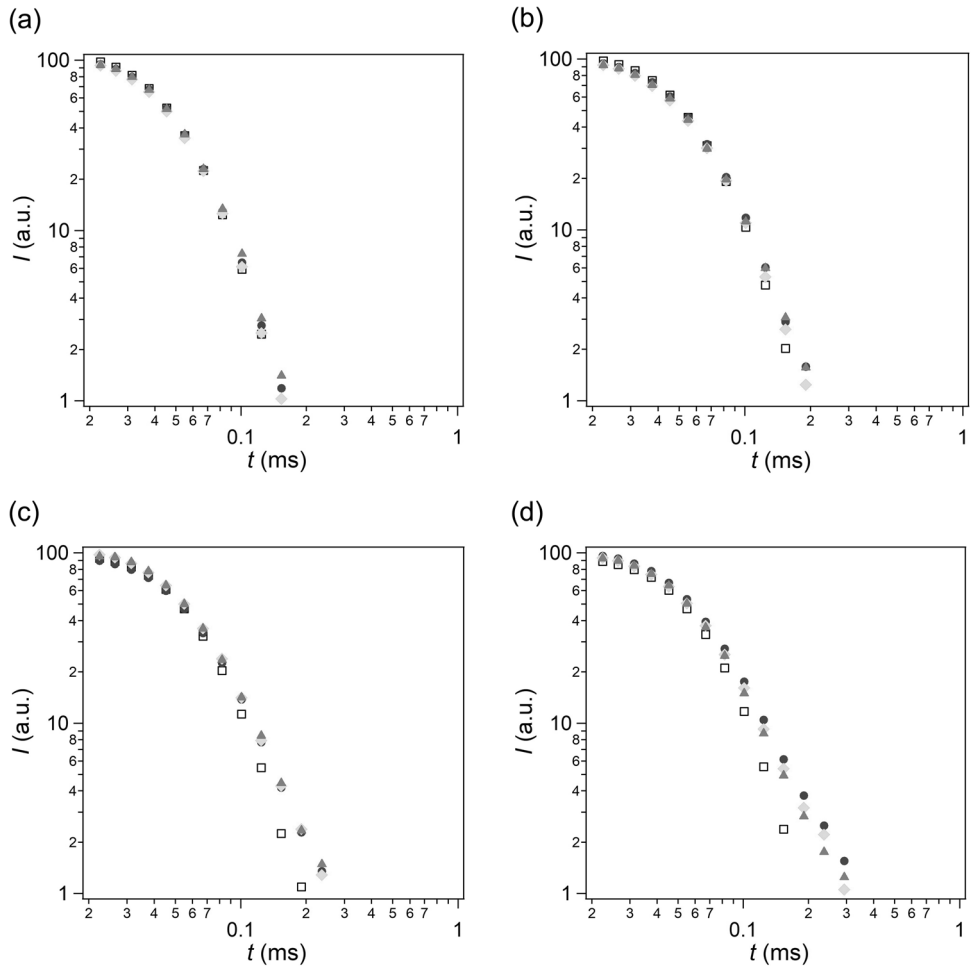

Fig. 8 FID profiles of the pulsed NMR measurements at (**a**) 30 °C, (**b**) 90 °C, (**c**) 120 °C, and (**d**) 150 °C for the neat epoxy (black), epoxy/PCL (blue), epoxy/PR 28 (green), and epoxy/PR09 (red) (Color figure online)

Pulsed NMR spectroscopy

To reveal the molecular origin of the unique viscoelastic relaxations of the epoxy resins with PRs, we studied the molecular dynamics of the samples by means of relaxation time measurements with pulsed NMR techniques. First, we compared the NMR results of the neat epoxy and epoxy/PCL to reveal the effect of the epoxy network on the chain dynamics of PCL. Figure 6 shows the obtained free induction decays (FIDs) for the neat epoxy and epoxy/PCL at 30 °C, 90 °C, 120 °C, and 150 °C. Since all the temperatures are below the T_g of the neat epoxy, the FIDs of the neat epoxy resin correspond to the local molecular motion of the glassy epoxy network. At 30 °C and 90 °C, the FIDs of epoxy/PCL completely overlap with that of the neat epoxy. This suggests that the PCL in epoxy/PCL is in the glassy state and its chain dynamics are similar to the local motion of the epoxy network, even though the temperatures of 30 °C and 90 °C are much higher than the T_g of neat PCL, −50 °C [12]. At 120 °C, the FID of epoxy/PCL deviates from that of the neat epoxy at times longer than 0.1 ms. The longer relaxation mode of epoxy/PCL becomes more obvious at 150 °C.

For a more quantitative analysis, the relaxation times were estimated by fitting the FIDs. For the neat epoxy resin and epoxy/PCL below 90 °C, the decay functions were well fitted by the sum of two Gaussian components [32]:

$$I = A_1 \exp(-t/T_1)^2 + A_2 \exp(-t/T_2)^2 \quad (1)$$

where T_i ($i = 1, 2$) is the relaxation time, and A_i is ($i = 1, 2$) the amplitude of each relaxation mode. For epoxy/PCL above 120 °C, another component corresponding to the longest relaxation mode needed to be added:

$$I = A_1 \exp(-t/T_1)^2 + A_2 \exp(-t/T_2)^2 + A_3 \exp(-t/T_3) \quad (2)$$

The temperature dependences of T_i and A_i/A_{total} ($=A_1 + A_2 + A_3$) for the neat epoxy and epoxy/PCL are shown in

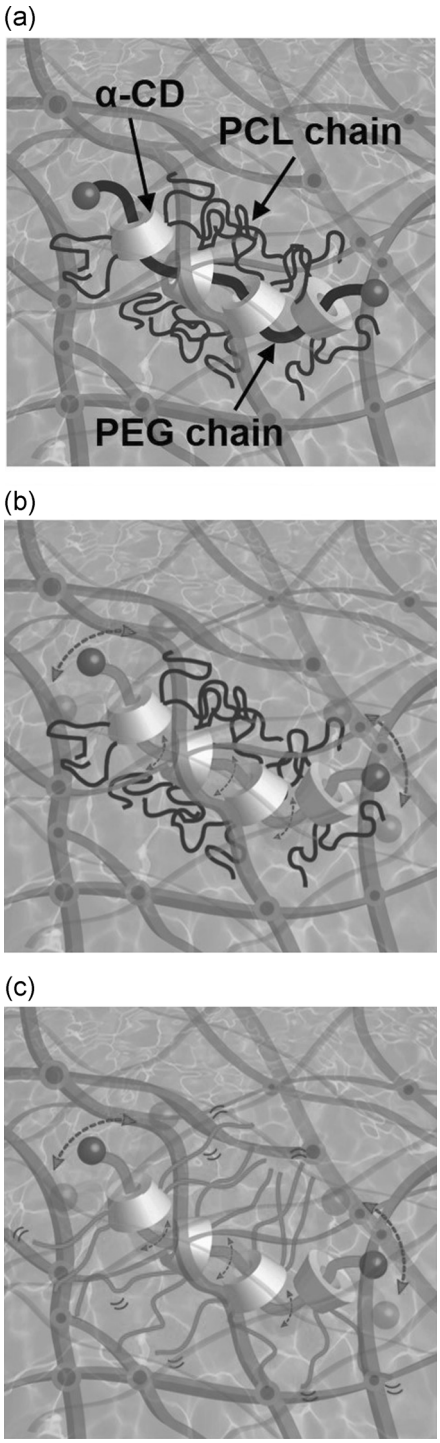

Fig. 9 Schematics of PR28 confined in the epoxy network: (**a**) low-temperature regime (below 60 °C), (**b**) intermediate temperature regime (from 60 °C to 120 °C), and (**c**) high temperature regime (above 120 °C)

Fig. 7a–c. The relaxation times of the neat epoxy remained constant or increased slightly with increasing temperature, but the temperature dependence is very weak. In the measured temperature range, the epoxy network is in the glassy state, which means that the local dynamics are restricted. For epoxy/PCL, the shorter relaxation times T_1 and T_2 are almost the same as those of the neat epoxy at all temperatures, and a longer relaxation time T_3 appears above 120 °C. The fraction of the longest relaxation mode, A_3/A_{total}, is ~10%, which is close to the fraction of protons of PCL in epoxy/PCL, 10%. The shorter relaxation times T_1 and T_2 can be attributed to the dynamics of the epoxy network in epoxy/PCL, while the longest relaxation time T_3 above 120 °C was assigned to the chain dynamics of PCL. PCL confined in the epoxy network shows a glass-rubber transition starting at 120 °C, which is the origin of the increase in tanδ observed in the DMA measurements starting at 100 °C (Fig. 5c). Interestingly, the onset temperature of the glass-rubber transition for PCL in the epoxy network, 120 °C, is much higher than that of the neat PCL, −50 °C (Fig. S9). In addition, T_3 of PCL in the epoxy network in the temperature range of 120–210 °C is 0.1–0.3 ms and is much shorter than the relaxation time of the neat PCL at the same temperatures, 3–8 ms (Fig. S9). The large shift in the glass transition temperature (T_g) and T_3 relaxation time for PCL suggests the strong confinement of PCL in the nanoscale epoxy network. On the other hand, the shorter T_1 and T_2 relaxation times of the epoxy network are not influenced by the addition of PCL even at temperatures higher than the T_g of PCL. This implies that PCL is not miscible in the epoxy network. During the curing reaction, the confinement of PCL via the cross-linked epoxy network suppresses the phase separation between the epoxy and PCL, which leads to the homogeneous dispersion of PCL in the epoxy network.

Next, the molecular dynamics of PR28 and PR09 in the epoxy networks were studied using pulsed NMR spectroscopy. Since the fractions of protons on PEG in epoxy/PR28 and epoxy/PR09 are <1%, pulsed NMR cannot detect the dynamics of PEG, but it can elucidate those of the epoxy network and PCL-grafted CDs. As shown in Fig. 8, the FIDs of epoxy/PR28 and epoxy/PR09 overlap with that of epoxy/PCL and deviate from that of the neat epoxy resin at temperatures above 120 °C. The long relaxation mode observed above 120 °C is attributable to the confined chain dynamics of the PCL graft chains in PR28 and PR09. Below 120 °C, the PCL graft chains are in the glassy state, and the chain dynamics are restricted. On the other hand, from the DMA results, epoxy/PR28 and epoxy/PR09 show viscoelastic relaxations attributable to PR dynamics above 60 °C and 20 °C, respectively, both of which are lower than the onset temperature of the glass-rubber transition for the PCL confined in the epoxy network, 120 °C. From these facts, we can conclude that the unique viscoelastic relaxation of PRs in the epoxy network originates from the PEG chain dynamics in PRs.

Figure 9a–c show schematics of the molecular dynamics in epoxy/PR28 in the three temperature regimes. At temperatures below 60 °C, both the PCL graft chains and PEG

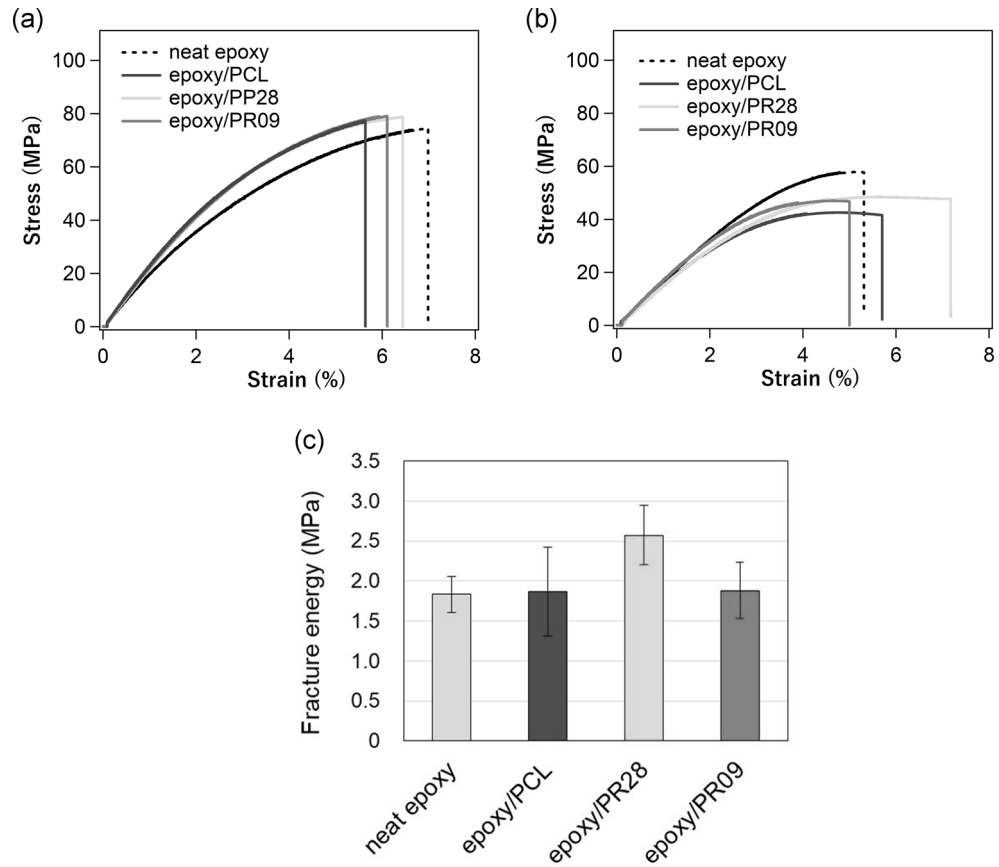

Fig. 10 Stress-strain curves (**a**) at room temperature and (**b**) 90 °C for the neat epoxy resin, epoxy/PCL, epoxy/PR28 and epoxy/PR09 and (**c**) fracture energies of the samples at 90 °C

in PR28 are in the glassy state, and their dynamics are almost the same as that of the epoxy matrix (Fig. 9a). In the intermediate temperature regime of 60 °C to 120 °C, PEG chains fluctuate in the glassy PCL-grafted CDs and epoxy networks (Fig. 9b), which causes a peculiar viscoelastic relaxation. Above 120 °C, the PCL graft chains also start fluctuating in the epoxy framework (Fig. 9c), corresponding to the long relaxation time T_3. The reduction in the coverage of PR from 28% to 9% decreases the onset temperature of the glass-rubber transition of PEG from 60 °C to 20 °C.

In the epoxy network, the onset temperatures of the glass-rubber transition for PEG in epoxy/PR28 and epoxy/PR09 are estimated to be 60 °C and 20 °C, respectively, which are much higher than the T_g of neat PEG, −50 °C [16]. It is worth noting that the T_g of PEG in PR glasses with a CD coverage of 28% (Fig. 1a) is almost the same as that of neat PEG [17]. Although the chain dynamics of neat PEG are restricted by the presence of crystalline PEG domains and PEG in PR glasses is confined by the glassy CD framework, the PEG dynamics in epoxy/PR28 and PR09 are more suppressed than those in neat PEG and PR glasses. For epoxy/PR28 and PR09, PEG is surrounded by CDs with glassy PCLs strongly constrained by the epoxy network. The confinement effect of the cross-linked epoxy network on the dynamics of PR is mainly responsible for the higher T_g of PEG in epoxy/PR28 and epoxy/PR09 than that of neat PEG and PEG in PR glasses. In addition, the coverage of PR substantially influences the T_g of PEG in epoxy resins with PRs. Decreasing the coverage of PR drastically enhances the axial PEG chain dynamics even in the glassy epoxy network. This may be because the free volume for PEG in the PRs increases with decreasing CD coverage. Detailed dynamics in PRs confined by epoxy networks will be studied in a future work.

Tensile tests

Finally, we evaluated the mechanical toughness of the epoxy resins by uniaxial tensile tests. At room temperature, as shown in Fig. 10a, the addition of PCL, PR28, and PR09 has no significant effects on the stress-strain curves of the epoxy resin. Although PEG in epoxy/PR09 fluctuates at room temperature, the strength of the viscoelastic relaxation caused by the PEG dynamics may not be enough to enhance the mechanical toughness. Figure 10b shows the tensile test results of the samples at 90 °C, which is higher than the

onset temperature of the glass-rubber transition of PEG in epoxy/PR28. Only epoxy/PR28 exhibits a higher strain at break than the neat epoxy resin. The fracture energies calculated from the areas under the stress-strain curves at 90 °C are summarized in Fig. 10c. The fracture energy of epoxy/PR28 is larger than those of the other materials, which indicates that the enhanced fracture toughness is related to the viscoelastic relaxation ascribed to the PEG dynamics in PR28. For further toughening, it would be important to strengthen the interfacial interactions between the PRs and the epoxy matrix by introducing chemical cross-links.

Conclusions

In this study, the molecular dynamics of PCL-grafted PRs homogeneously dispersed in a cross-linked epoxy network were investigated using viscoelastic mechanical measurements and relaxation time measurements with pulsed NMR spectroscopy. With increasing temperature, the PEG chains in the PRs exhibit a glass-rubber transition and start fluctuating in the CDs with glassy PCL graft chains, which causes viscoelastic mechanical relaxation. The glass transition temperature (T_g) of PEG in the epoxy resins containing PRs is much higher than that of neat PEG, which indicates that PR is strongly confined by the glassy epoxy network. Another dominant factor influencing the T_g of PEG in PR confined by the epoxy network is the coverage of CDs on PEG in PR. The mobility of the axial PEG chain is drastically changed by the confinement effect of the epoxy network and the topological constraints of the PCL-grafted CDs. The viscoelastic relaxation derived from PEG dynamics in PR increases the stretchability and mechanical toughness of the epoxy resin under uniaxial deformation. These findings provide a clear strategy for controlling the temperature/frequency regime for the viscoelastic relaxation attributed to PR dynamics over a wide range and enhancing the mechanical toughness of epoxy resins by the introduction of PRs.

Acknowledgements This work was supported by JST-Mirai Program Grant Number JPMJMI18A2. The authors would like to thank Dr Lan Jiang and Mr Yohei Iwahashi for the preparation of PR09, Mr Jun Ito for the TEM observations of a series of cured samples, and Dr Masanobu Naito and Dr Sadaki Samitsu for the helpful discussions.

Compliance with ethical standards

Conflict of interest The authors declare that they have no conflict of interest.

References

1. Sauvage JP, Dietrich-Buchecker C. Molecular catenanes, rotaxanes, and knots. Weinheim: Wiley–VCH; 1999.
2. Harada A, Hashidzume A. Takashima Y. Cyclodextrin-based supramolecular polymers. In: Supramolecular polymers polymeric betains oligomers. Springer, Berlin, Heidelberg, 2006. pp. 1–43.
3. Wenz G, Han BH, Muller A. Cyclodextrin rotaxanes and polyrotaxanes. Chem Rev. 2006;106:782–817.
4. Takata T, Kihara N, Furusho Y. Polyrotaxanes and polycatenanes: recent advances in syntheses and applications of polymers comprising of interlocked structures. Adv Polym Sci. 2004;171:1–75.
5. Ito K, Kato K, Mayumi K. Polyrotaxane and slide-ring materials. Royal Society of Chemistry; Cambridge, UK, 2015.
6. Yasuda Y, Hidaka Y, Mayumi K, Yamada T, Fujimoto K, Okazaki S, et al. Molecular dynamics of polyrotaxane in solution investigated by quasi-elastic neutron scattering and molecular dynamics simulation: sliding motion of rings on polymer. J Am Chem Soc. 2019;141:9655–63.
7. Nepogodiev SA, Stoddart JF. Cyclodextrin-based catenanes and rotaxanes. Chem Rev. 1998;98:1959–76.
8. Okumura Y, Ito K. The polyrotaxane gel: a topological gel by figure-of-eight cross-links. Adv Mater. 2001;13:485–7.
9. Ito K. Novel cross-linking concept of polymer network: synthesis, structure, and properties of slide-ring gels with freely movable junctions. Polym J. 2007;39:489–99.
10. Liu C, Kadono H, Mayumi K, Kato K, Yokoyama H, Ito K. Unusual fracture behavior of slide-ring gels with movable cross-links. ACS Macro Lett. 2017;6:1409–13.
11. Sawada J, Aoki D, Uchida S, Otsuka H, Takata T. Synthesis of vinylic macromolecular rotaxane cross-linkers endowing network polymers with toughness. ACS Macro Lett. 2015;4:598–601.
12. Minato K, Mayumi K, Maeda R, Kato K, Yokoyama H, Ito K. Mechanical properties of supramolecular elastomers prepared from polymer-grafted polyrotaxane. Polymer. 2017;128:386–91.
13. Koyanagi K, Takashima Y, Yamaguchi H, Harada A. Movable cross-linked polymeric materials from bulk polymerization of reactive polyrotaxane cross-linker with acrylate monomers. Macromolecules. 2017;50:5695–700.
14. Gotoh H, Liu C, Imran AB, Hara M, Seki T, Mayumi K, et al. Optically transparent, high-toughness elastomer using a polyrotaxane cross-linker as a molecular pulley. Sci Adv. 2018;4:eaat7629.
15. Kato K, Mizusawa T, Yokoyama H, Ito K. Polyrotaxane glass: peculiar mechanics attributable to the isolated dynamics of different components. J Phys Chem Lett. 2015;6:4043–8.
16. Kato K, Mizusawa T, Yokoyama H, Ito K. Effect of topological constraint and confined motions on the viscoelasticity of polyrotaxane glass with different interactions between rings. J Phys Chem C. 2017;121:1861–9.
17. Kato K, Ohara A, Yokoyama H, Ito K. Prolonged glass transition due to topological constraints in polyrotaxanes. J Am Chem Soc. 2019;141:12502–6.
18. Wang XS, Kim HK, Fujita Y, Sudo A, Nishida H, Endo T. Relaxation and reinforcing effects of polyrotaxane in an epoxy resin matrix. Macromolecules. 2006;39:1046–52.
19. Li X, Kang HL, Shen JX, Zhang LQ, Nishi T, Ito K. Miscibility, intramolecular specific interactions and mechanical properties of a DGEBA based epoxy resin toughened with a sliding graft copolymer. Chin J Polym Sci. 2015;33:433–43.
20. Pruksawan S, Samitsu S, Yokoyama H, Naito M. Homogeneously dispersed polyrotaxane in epoxy adhesive and its improvement in the fracture toughness. Macromolecules. 2019;52:2464–75.

21. Seo J, Yui N, Seo JH. Development of a supramolecular accelerator simultaneously to increase the cross-linking density and ductility of an epoxy resin. Chem Eng J. 2019;356:303–11.
22. Henghua J, Gina MM, Stephen JP, Anthony SG, Dylan SS, Dennis R, et al. Fracture behavior of a self-healing, toughened epoxy adhesive. Int J Adhes Adhesives. 2013;44:157–65.
23. Mimura K, Ito H, Fujioka H. Improvement of thermal and mechanical properties by control of morphologies in PES-modified epoxy resins. Polymer. 2000;41:4451–9.
24. Meier U. Strengthening of structures using carbon fibre/epoxy composites. Constr Build Mater. 1995;9:341–51.
25. Kato K, Hori A, Ito K. An efficient synthesis of low-covered polyrotaxanes grafted with poly (ε-caprolactone) and the mechanical properties of its cross-linked elastomers. Polymer. 2018;147:67–73.
26. Challis RE, Freemantle RJ, Cocker RP, Chadwick DL, Dare DJ, Martin C, et al. Ultrasonic measurements related to evolution of structure in curing epoxy resins. Plast, Rubber Compos. 2000;29:109–18.
27. Detwiler AT, Lesser AJ. Characterization of double network epoxies with tunable compositions. J Mater Sci. 2012;47:3493–503.
28. Lovell R, Windie AH. WAXS investigation of local structure in epoxy networks. Polymer. 1990;31:593–601.
29. Takahama T, Geil PH. The β relaxation behavior of bisphenol-type resins. J Polym Sci, Polym Phys Ed. 1982;20:1979–86.
30. Grillet AC, Galy J, Gérard JF, Pascault JP. Mechanical and viscoelastic properties of epoxy networks cured with aromatic diamines. Polymer. 1991;32:1885–91.
31. Ochi M, Okazaki M, Shimbo M. Mechanical relaxation mechanism of epoxide resins cured with aliphatic diamines. J Polym Sci: Polym Phys Ed. 1982;20:689–99.
32. Kimoto H, Tanaka C, Yaginuma M, Shinohara E, Asano A, Kurotsu T. Pulsed NMR study of the curing process of epoxy resin. Anal Sci. 2008;24:915–20.